Rear-surface light intensification caused by Hertzian-conical crack in 355-nm silica optics*

Zhang Chun-Lai(章春来)[a], Yuan Xiao-Dong(袁晓东)[b], Xiang Xia(向 霞)[a)†], Wang Zhi-Guo(王治国)[a], Liu Chun-Ming(刘春明)[a)b)], Li Li(李 莉)[a], He Shao-Bo(贺少勃)[a)b)], and Zu Xiao-Tao(祖小涛)[a]

[a] *School of Physical Electronics, University of Electronic Science and Technology of China, Chengdu* 610054, *China*
[b] *Research Center of Laser Fusion, China Academy of Engineering Physics, Mianyang* 621900, *China*

(Received 1 January 2012; revised manuscript received 17 March 2012)

Theoretical studies show that the Hertzian-conical crack can be considered to be composed of double cone faces for simplification. In the present study, the three-dimensional finite-difference time-domain method is employed to quantify the electric-field distribution within the subsurface in the presence of such a defect under the normal incidence irradiation. Both impurities (inside the crack) and the chemical etching have been investigated. The results show that the maximum electric field amplitude $|E|_{\max}$ is 9.57374 V/m when the relative dielectric constant of transparent impurity equals 8.5. And the near-field modulation will be improved if the crack filled with remainder polishing powders or water vapor/drops. Meanwhile, the laser-induced initial damage is moving to the glass–air surface. In the etched section, the magnitude of intensification is strongly dependent on the inclination angle θ. There will be a highest modulation when θ is around $\pi/6$, and the maximum value of $|E|_{\max}$ is 18.57314 V/m. When θ ranges from $\pi/8$ to $\pi/4$, the light intensity enhancement factor can easily be larger than 100, and the modulation follows a decreasing trend. On the other hand, the modulation curves become smooth when $\theta > \pi/4$ or $\theta < \pi/8$.

Keywords: fused silica, wet etching, Hertzian-conical crack, finite-difference time-domain method

PACS: 42.60.Jf, 42.62.–b, 42.70.Ce, 52.57.–z **DOI:** 10.1088/1674-1056/21/9/094213

1. Introduction

Nowadays, improving the laser-induced damage resistance is still a great technological challenge, particularly at 355-nm high power output systems, such as the Laser Méga Joule and the National Ignition Facility.[1,2] In high-power laser systems, light intensity modulations caused by impurities and cracks on silica subsurfaces often increase the possibility for laser-induced damage.[1,3,4] The typical impurities include polishing compound components (e.g., CeO_2 and ZrO_2) and metals (e.g., Pt, Fe, Cu, and Cr) induced during the polishing steps or the earlier grinding steps.[3] According to the fracture geometry and indentation, subsurface cracks can be divided into Hertzian-conical crack (HCC), radial crack, lateral crack, trailing Hertzian indent, and so on.[5,6] The silica optics are usually etched by the HF acid to improve the laser induced damage threshold.[7,8] The cracks will be passivated and transformed into different morphologies during the erosion process, which has been used for the mitigation of laser damage growth by Bouchut *et al.*[8] and Hrubesh *et al.*[9]

The HCC plays an important role in the field-induced damage, especially when it locates at the output surface.[6] Génin *et al.* reported that the light intensity enhancement factor (LIEF) is about 2 orders of magnitude near the HCC region.[10] Hua *et al.* has simulated the light intensity distributions in the vicinity of three-dimensional (3D) HCCs with different sizes, and showed some advices for controlling the HCC size.[11] Up to now, most of the theoretical investigations of HCC focused on the light intensity modulation with a single variable, but not on the multivariable situations, such as the acid etching.[10,11] Meanwhile, the light intensification of HCC contained transparent impurities has not been reported.

In this work, we investigated the electric-field dis-

*Project supported by the Young Scientists Fund of the National Natural Science Foundation of China (Grant No. 10904008), the Joint Fund of the National Natural Science Foundation of China and the China Academy of Engineering Physics (Grant No. 11076008), and the Scientific Research Foundation for the Central Universities of China (Grant Nos. ZYGX2009X007, ZYGX2010J045, and ZYGX2011J043).

†Corresponding author. E-mail: xiaxiang@uestc.edu.cn

© 2012 Chinese Physical Society and IOP Publishing Ltd

tribution in the vicinity of HCC defects during the erosion process using the finite-difference time-domain (FDTD) method. The effects of near-field modulation of different transparent impurites inside the HCC have also been investigated. All of them may contribute to the laser induced damage initiation. The relationships between the maximum electric field amplitude ($|E|_{\max}$) in the fused silica and the etch value (or the relative dielectric constant $\varepsilon_{\rm r}$) are presented. The aim of this work is to understand the evolution of field-induced damage caused by the HCC defect during the manufacturing and the pretreatment processes of the fused silica.

2. Model and method

Figure 1(a) schematically shows the formation of a typical HCC on the fused silica sub-surface induced by a blunt ZrO_2 (CeO_2) particle upon polishing.[5,6] The force from the particle distributes on a near circular contact surface, and a symmetrical crack will be created when the deformation is beyond the elastic limit (see Figs. 1(a) and 1(b)). The width and the depth of the crack will be in the range from several μm to tens of μm after the acid etching (see Fig. 1(c)).

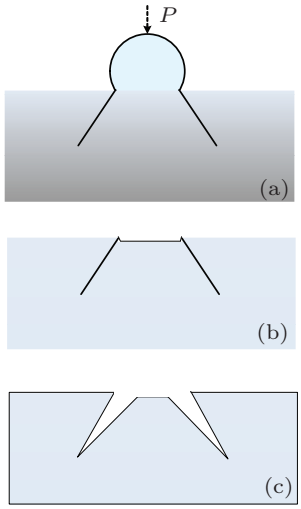


Fig. 1. Schematic illustrations of idealized HCC formation,[6] panel (a) shows the blunt indenter, panels (d) and (c) show cross-sectional views before and after the chemical etching, respectively.

The HCC is considered as the initiation position of laser-irradiation induced damage, especially at the output surface for the normal-incidence irradiation. Based on the morphologies shown in Fig. 1, we construct a simple mathematic model with absolute smooth surfaces to model the HCC, as shown in Fig. 2. The HCC is composed of two conical surfaces with colinear vertexes in the z direction, which has been mentioned by Génin *et al.*,[10] however, they did not explain it in detail. Assume the etching is isotropic and the coordinate of the symmetrical center on the glass–air surface is (x_0, y_0, z_0), then the inside and the outside cone surfaces can be respectively described by the following 3D equations:

$$z(x,y) = -\cot\theta\sqrt{(x-x_0)^2+(y-y_0)^2}+z_0 + \frac{r}{\tan\theta}-\frac{\Delta x}{\sin\theta}, \quad (1)$$

$$z(x,y) = \frac{d}{w-d\tan\theta}\sqrt{(x-x_0)^2+(y-y_0)^2}+z_0 + \frac{d(w+r)}{d\tan\theta-w}+\Delta x\sqrt{1+\left(\frac{d}{d\tan\theta-w}\right)^2}, \quad (2)$$

where all the parameters are presented in Fig. 2.

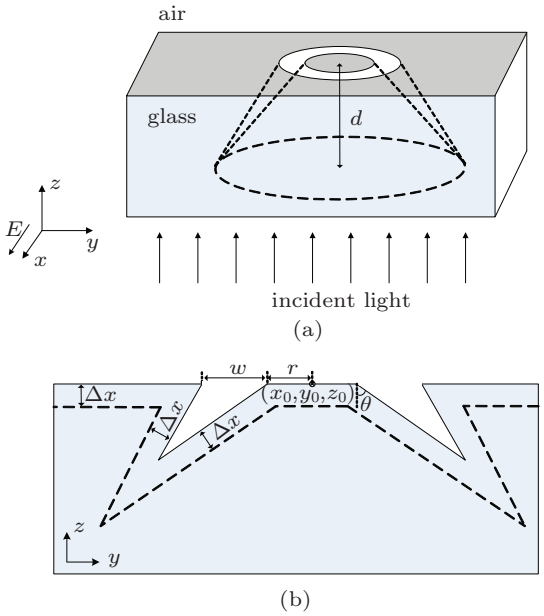


Fig. 2. Schematic diagrams of cone model. Panel (a) shows that the 3D HCC is constituted by two (inside and outside) conical surfaces and the air–glass surface is from the horizontal cross-section. The crack is on the output surface, where w, d, r, and θ refer to its width, depth, inside radius, and inclination angle, respectively. The light travels in the direction normal to the surface, and the direction of the electric field is indicated in panel (a). The HCC with etching is illustrated in panel (b), where the solid lines represent surfaces before etching, the dashed lines represent surfaces after etching, and Δx represents the etch value in the isotropic etching.

The etch model shown in Fig. 2(b) was firstly described in Ref. [6], which is based on the assumption that the etching occurs nearly isotropically for the opening HCC. By simple geometry calculation and assuming the isotropic etching, the width increment

(Δw) and the depth increment (Δd) of the fracture opening HCC with etch value Δx are given by

$$\Delta w = \frac{\Delta x}{\cos\theta} + \Delta x\sqrt{1+\left(\tan\theta - \frac{w}{d}\right)^2} - \frac{w\Delta x}{d}, \quad (3)$$

$$\Delta d = \frac{d\Delta x}{w\cos\theta} + \frac{d\Delta x}{w}\sqrt{1+\left(\tan\theta - \frac{w}{d}\right)^2} - \Delta x, \quad (4)$$

where θ is the angle of the crack relative to the vertical line. From Eqs. (3) and (4), we can see that there is a good linear relationship between Δw (or Δd) and Δx in the isotropic etching.

The FDTD method is employed to solve Maxwell's equations for the scattering of an electromagnetic plane wave in the vicinity of HCC. The simulation domain is 3D, rectangular, and gridded with a uniform grid of $\delta = \lambda/12$, where λ is the 355-nm laser wavelength. For the normal incidence irradiation, the electric field amplitude ($|E|$) of the incident light is 1.0 V/m, and the relative dielectric constants ($\varepsilon_{\rm r}$) of air and glass are 1.0 and 2.25, respectively.[11] The $\varepsilon_{\rm r}$ value inside the HCC is varied from 1.0 to 15.0 for the transparent impurities under investigation, and the crack is full of impurities for simplification. The $\varepsilon_{\rm r}$ value is 1.0 (filled with air) in the etched section. The periodic boundary conditions (PBC) are applied in the horizontal direction, while the Berenger's perfectly matched layer (PML) absorbing boundary condition is applied in the vertical direction.[12,13]

3. Results and discussion

3.1. Simulation of impurities

The HCC is filled with air. The electric field intensity profiles of the HCC are plotted by using a gray scale in Fig. 3, in which the lighter areas represent intense electric fields. We consider two illumination planes, in which the electric field is either perpendicular (transverse electric (TE) illumination) or parallel (transverse magnetic (TM) illumination) to the plane.[10,14] From Fig. 3, we can see that the distribution of electric field is symmetrical and the modulation of electric field is notable. The incident laser is scattered into the fused silica by the inside air–crack interface, and the multiple scattering waves overlap with the incident wave (see Figs. 3(a) and 3(b)). A standing wave is generated by these reflections, and high-intensity spots result from the constructive interference between these waves.[10,13] In the TE plane (Fig. 3(a)), $|E|_{\rm max}$ is 8.38449 V/m, and the high intensified area is larger than that in the TM plane (Fig. 3(b)). According to statistics, there are 1129 grid points with $|E| > 2.0$ V/m (intensified points, IPs) in the TE plane. However, the smaller $|E|_{\rm max}$ value and IPs of 7.88402 V/m and 241 respectively are found in the TM plane, as shown in Fig. 3(b). As can be seen from Fig. 3(c), all the bright points locate at the inside circle, and there are more IPs perpendicular to the E direction than parallel to it, which is consistent with the previous report.[10]

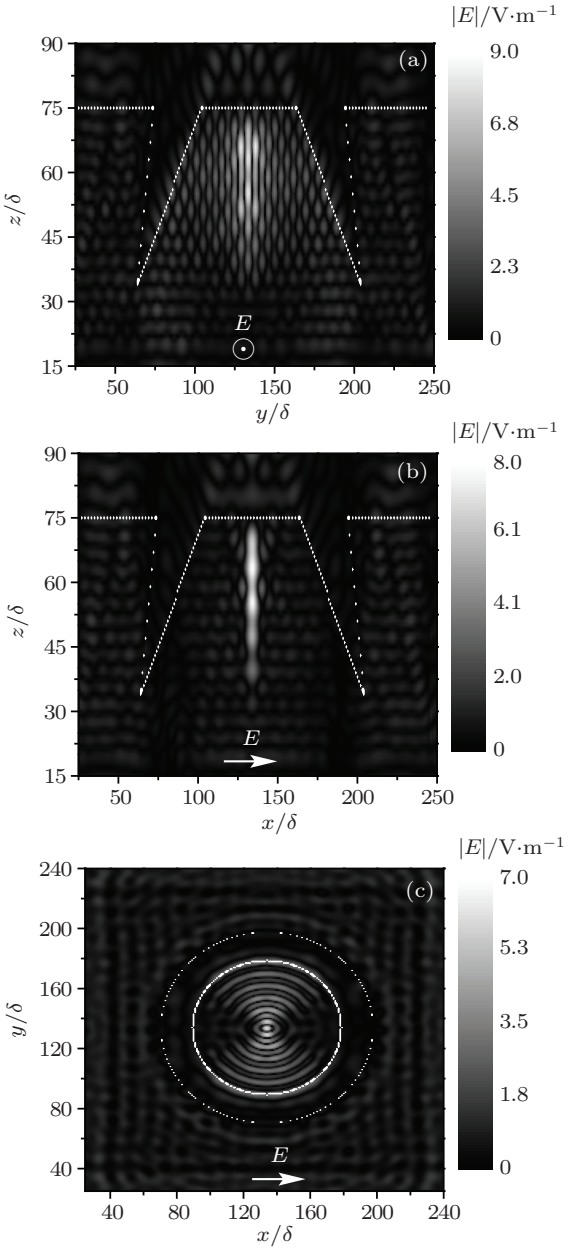


Fig. 3. Vertical ((a) TE and (b) TM planes) and horizontal ((c) plane view cut at $z = 60\delta$) cross sections of the electric field amplitude distribution for the HCC with $w = 30\delta$, $d = 40\delta$, $r = 30\delta$, and $\theta = \pi/4$. The air–glass surface is at $z = 75\delta$, and the size of the simulation domain is $250\delta \times 250\delta \times 90\delta$.

Figures 4(a) and 4(b) show the simulation results of HCC filled with variable transparent impurities with their ε_r varying from 1.0 to 15.0. It can be seen that the trends of the four curves with ε_r are similar. Both $|E|_{max}$ and IPs decrease with increasing ε_r up to 2.25, and then increase firstly and decrease later as ε_r further increases beyond 2.25. As can be seen from Fig. 4(a), the values of $|E|_{max}$ in TE and TM planes are close to each other, and reach the same peak value of 9.57374 V/m at $\varepsilon_r = 8.5$. In Fig. 4(b), there are remarkable differences between the results in TE and TM planes except for $1.5 < \varepsilon_r < 3.0$. It is indicated that a larger modulation is presented in the TE plane than that in the TM plane, which is consistent with the results obtained by comparing Fig. 3(a) with Fig. 3(b). The values of ε_r for the standard polishing powders ZrO_2 and CeO_2 are 4 and 5.3 ($\varepsilon_r \approx n^2$,[15,16] where n is the refractive index, for ZrO_2 and CeO_2, the indexes are 2.0 and 2.3,[3] respectively), respectively. The corresponding values of $|E|_{max}$ are 5.60910 V/m and 7.86745 V/m in the TM plane, which are smaller than the value of 8.38449 V/m when the crack is filled with air. Thus, the effect of remainder polishing powders left on the output crack–air interface can be neglected when considering the near-field modulation. Moreover, the modulation of most impurities can be neglected except ε_r is around 8.5, as shown in Fig. 4(a).

We can see from Figs. 5(a) and 5(b) that the high electric field distribution area becomes more and more narrow with ε_r closing to 2.25, and the transmission from the crack becomes much stronger. It is corresponding to the cracks filled with water drops or water vapor after the chemical etching or caused by humid air. And the modulation becomes weaker compared to that in Fig. 3(a). Further increasing ε_r, as shown in Figs. 5(c)–5(f), the high-intensity spots approach the air–glass surface, which is called the skin effect determined by the interface reflection. Additionally, the transmission coming from the air–crack interface becomes stronger proved by the brighter impurity spots, which also follows the principles of optics. Now, let us answer why $|E|_{max}$ increases firstly and then decreases when $\varepsilon_r > 2.25$. In Fig. 4(c), α and β are fixed for given HCC, incident ray a, and impurity. Calculated using the relationship of triangle, the incident angle of ray c is $\alpha+\beta$, then we can obtain the incident angle of ray d, which is $2\alpha+\beta$. Clearly, $2\alpha+\beta$ is greater than β at the inside interface (see Fig. 4(c)). According to the reversibility of the path of light transmitting through the media interface and the law of refraction, the angle between ray e and the interface will be less than θ, which means the interference derived from ray e is closer to the air–glass surface than that from ray b. We know, with increasing ε_r, ray c becomes stronger, and there must be a corresponding weaker ray b and a stronger ray e. So intensity spots approaching the surface result from the shift of the stronger reflection beam. When the reflection occurs at a proper angle ($\varepsilon_r = 8.5$), the constructive interference is best constructed, the $|E|_{max}$ peak appears. On the other hand, ray g will be stronger if ε_r keeps increasing, then ray e is too weak to obtain a high interference intensity. The proper ε_r is determined by the sizes of HCC. So it can be comprehended according to the whole self-consistent information.

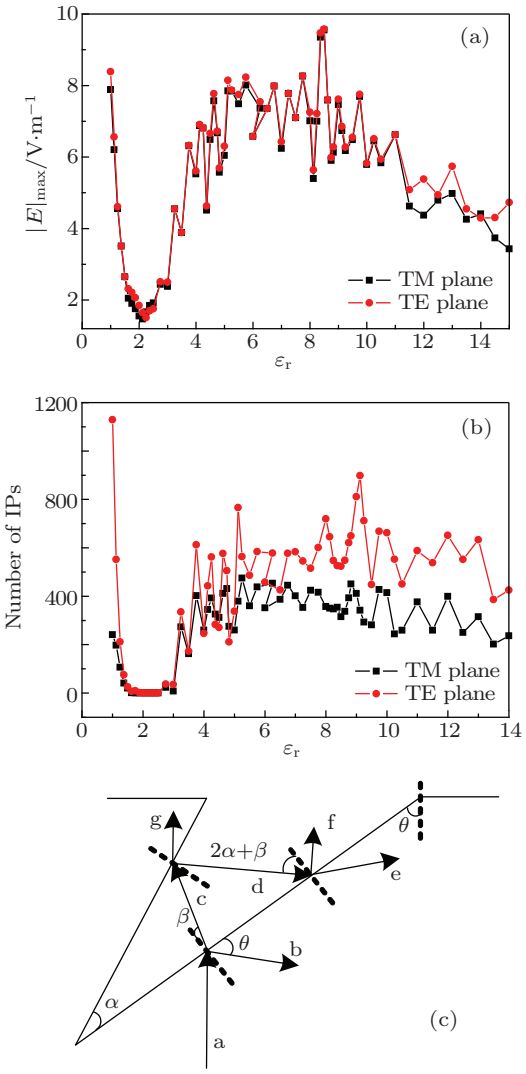


Fig. 4. (colour online) The (a) $|E|_{max}$ and (b) number of IPs each as a function of ε_r of the transparent impurities, the simulation parameters are the same as those in Fig. 3. Panel (c) shows schematically the reflection and refraction at the interfaces, where a, b, c, d, e, f, and g represent the rays, and α, β, and θ represent the angles.

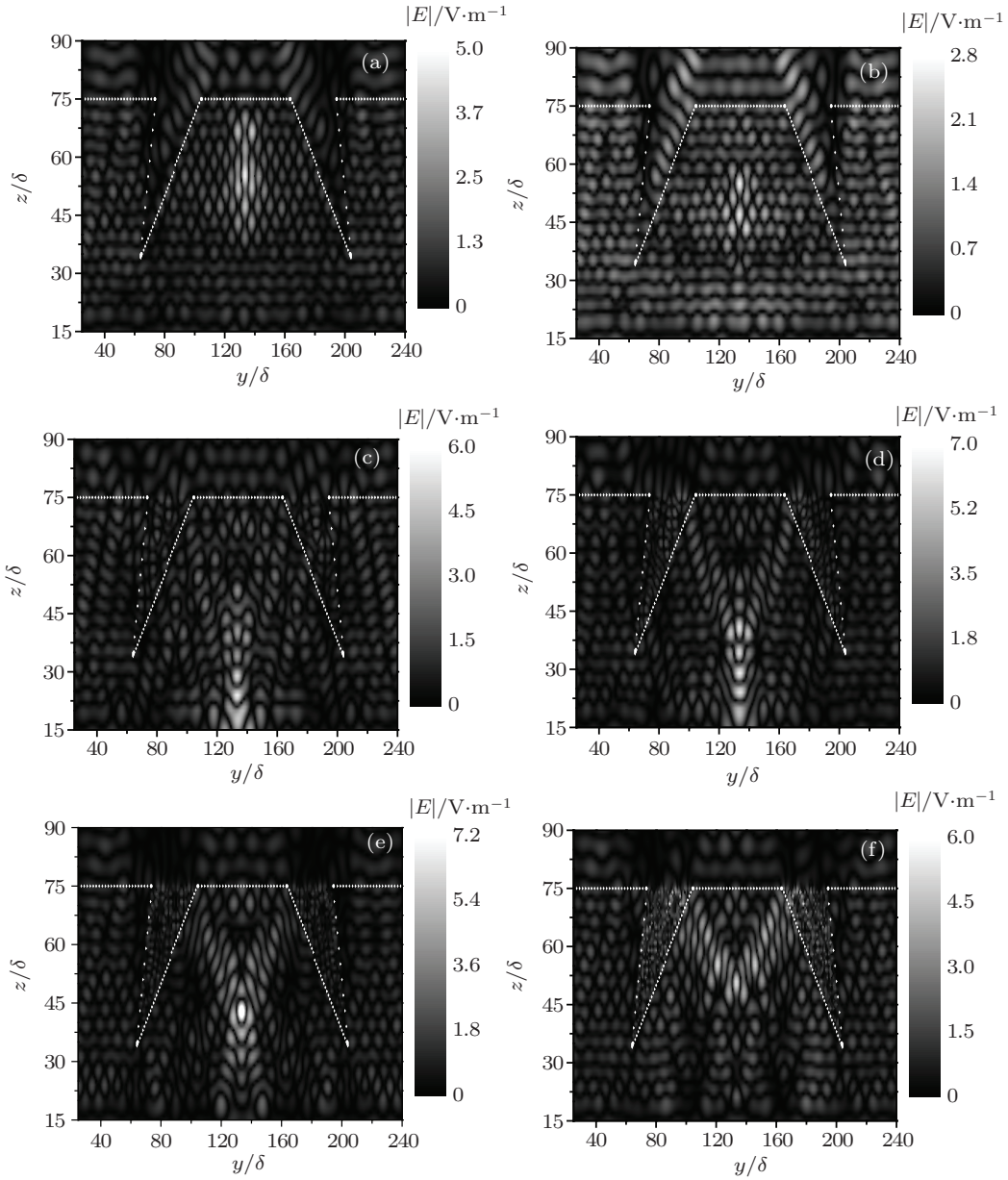


Fig. 5. Electric field amplitude distributions in the vicinity of cone cracks filled with transparent impurities with (a) $\varepsilon_{\rm r} = 1.25$, (b) $\varepsilon_{\rm r} = 1.5$, (c) $\varepsilon_{\rm r} = 4.0$, (d) $\varepsilon_{\rm r} = 6.0$, (e) $\varepsilon_{\rm r} = 8.5$, and (f) $\varepsilon_{\rm r} = 13.0$.

3.2. Simulation of chemical etching

Figure 6 shows the localized field enhancement near an output surface of HCC illuminated at normal incidence during the etching process. The maximum intensification is located between the middles of cone edges, which are delineated by dotted white lines. And it is found that there is no obvious change for a larger Δx. In order to simulate the realistic situation, the theoretical simulation is performed with the inclination angle changing from $\pi/9$ to $\pi/3$. Figure 7 shows the $|E|_{\rm max}$ distribution as a function of Δx with the same other simulation parameters. Considering θ as a variable, the field modulation gradually ascends to a peak when θ is increased to $\pi/6$, and then gradually declines when $\theta > \pi/6$. For different Δx, the maximum intensification on the subsurface varies in a wide range, for example, from as low as 3.97866 V/m to as high as 18.57314 V/m for $\theta = \pi/6$, which means that for a given cone angle, the maximum intensification spot always vibrates with the increasing Δx. Moreover, the modulation curves follow a decreasing trend for $\pi/8 < \theta < \pi/4$. As shown in Fig. 7, the curves become smooth when $\theta > \pi/4$ or $\theta < \pi/8$, especially when θ is $\pi/3$. On the other hand, some of these inclination angles around $\pi/6$ can easily induce

damage under further laser irradiation, and thus eventually limit the mirror performance and lifetime. The electric-field intensification strength within the domain is usually quantified by the normalized electric-field intensity or the square of the electric field,[12,13] which is also called the light intensity enhancement factor (LIEF).[3] From Fig. 7, we can see the LIEF can easily be larger than 100 when $\pi/8 < \theta < \pi/4$.

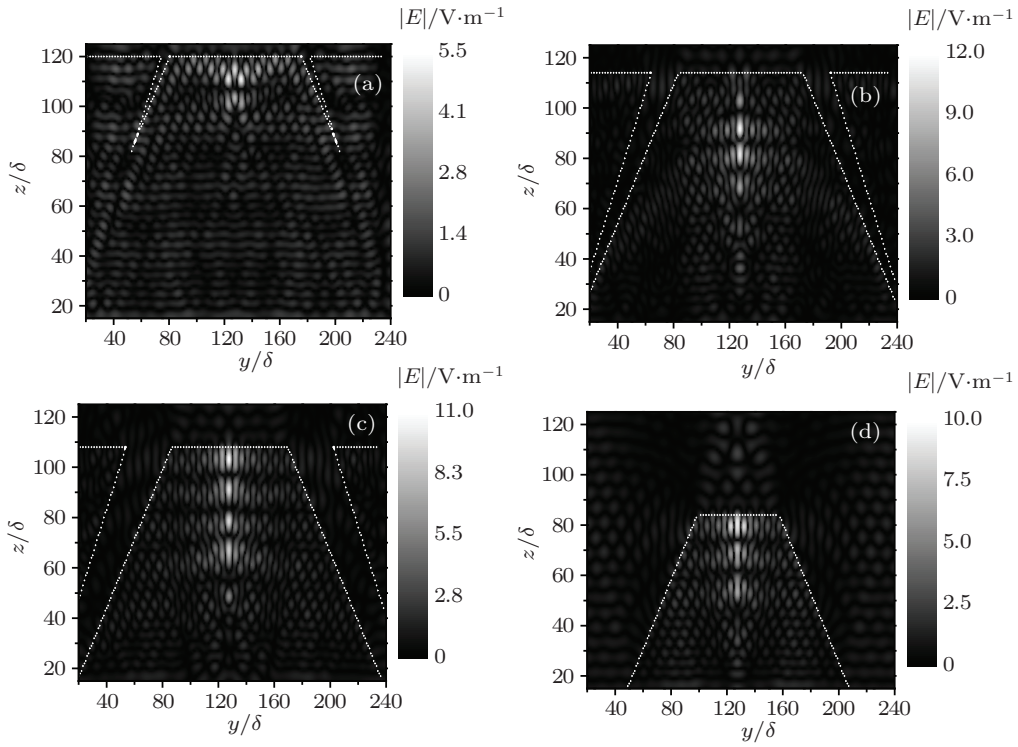


Fig. 6. Relationships between electric field amplitude distribution and chemical etch value ((a) $\Delta x = 0$; (b) $\Delta x = 6\delta$; (c) $\Delta x = 12\delta$; (d) $\Delta x = 36\delta$) of an original HCC with $w = 6\delta$, $d = 36\delta$, $r = 48\delta$, and $\theta = \pi/5$. The original air–glass surface is at $z = 120\delta$, and the size of the simulation domain is $240\delta \times 240\delta \times 125\delta$.

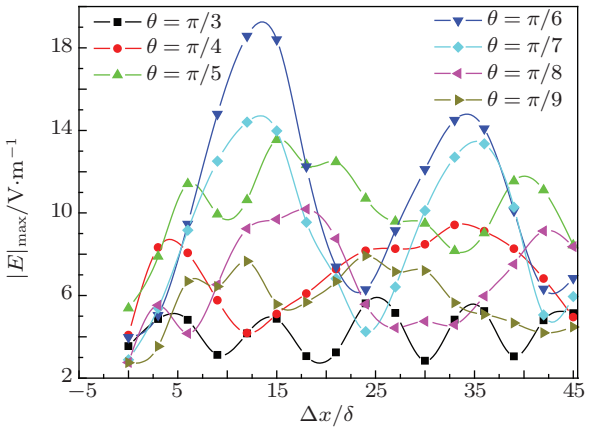


Fig. 7. (colour online) The maximum electric field amplitude as a function of etch value in the TE plane.

In summary, in order to avoid serious damages, we should get rid of the HCC with $\pi/8 < \theta < \pi/4$. The chemical etching may be used to reduce its local modulation at a certain extent for the aforementioned cracks, and there is no distinct change on the field enhancement after the etching when θ is larger than $\pi/4$ or smaller than $\pi/8$. For θ equaling $\pi/3$, the maximal electric field amplitude curve becomes lower and smoother.

4. Conclusions

In this paper, we have investigated the conical cracks using an ideal model composed of two conical surfaces and studied the light field modulation with the FDTD method. The simulation results show that the conical pits can generate high electric field intensification near the output surface illuminated at the normal incidence. The main conclusions are as follows.

1) If the crack is filled with transparent impurities, the enhancement of electric field intensity is decreased for ε_r increasing upto 2.25, and then $|E|_{max}$ increases firstly and decreases later as ε_r further increases beyond 2.25. Meanwhile, the whole intensity spots move close to the air–glass surface for the lat-

ter. The $|E|_{\max}$ values are close to each other in TE and TM planes, and have the same peak value of 9.57374 V/m at $\varepsilon_{\rm r} = 8.5$. The results have shown that the TE plane has more high-intensity spots than the TM plane. In addition, the near-field modulation is not seriously deteriorated when the crack is full of remainder polishing powders (e.g., CeO_2 and ZrO_2) or water drops/vapor.

2) The magnitude of the light field intensification is strongly dependent on the inclination angle during the chemical etching. The highest modulation occurs when $\theta \approx \pi/6$, the maximum value of $|E|_{\max}$ is 18.57314 V/m. When $\pi/8 < \theta < \pi/4$, the LIEF can easily be larger than 100, and the modulation becomes weaker with further etching. On the other hand, the modulation curves become smooth when $\theta > \pi/4$ or $\theta < \pi/8$, especially when θ is around $\pi/3$.

References

[1] Génin F Y, Feit M D, Kozlowski M R, Rubenchik A M, Salleo A and Yoshiyama J 2000 *Appl. Opt.* **39** 3654

[2] Li C H, Ju X, Jiang X D, Huang J, Zhou X D, Zheng Z, Wu W D, Zheng W G, Li Z X, Wang B Y and Yu X H 2011 *Opt. Express* **19** 6439

[3] Wang F R, Liu H J, Huang J, Zhou X D, Jiang X D, Wu W D, Zheng W G and Ju X 2011 *Chin. Phys. Lett.* **28** 014206

[4] Zhang C L, Li X B, Wang Z G, Liu C M, Xiang X, Lv H B, Yuan X D and Zu X T 2011 *Chin. Phys. Lett.* **28** 074205

[5] Suratwala T, Wong L, Miller P, Feit M D, Menapace J, Steele R, Davis P and Walmer D 2006 *J. Non-Cryst. Solids* **352** 5601

[6] Wong L, Suratwala T, Feit M D, Miller P E and Steele R 2009 *J. Non-Cryst. Solids* **355** 797

[7] Chen M, Xiang X, Jiang Y, Zu X T, Yuan X D, Zheng W G, Wang H J, Li X B, Lv H B, Jiang X D and Wang C C 2010 *High Power Laser and Part. Beams* **22** 1383 (in Chinese)

[8] Bouchut P, Garrec P and Pelle C 2003 *Proc. SPIE* **4932** 103

[9] Hrubesh L W, Norton M A, Molander W A, Wegner P J, Staggs M, Demos S G, Britten J A, Summers L J, Lindsey E F and Kozlowski M R 2001 *Proc. SPIE* **4374** 553

[10] Génin F Y, Salleo A, Pistor T V and Chase L L 2001 *J. Opt. Soc. Am.* A **18** 2607

[11] Hua J R, Zu X T, Li L, Xiang X, Chen M, Jiang X D, Yuan X D and Zheng W G 2010 *Acta Phys. Sin.* **59** 2519 (in Chinese)

[12] Qiu S R, Wolfe J E, Monterrosa A M, Feit M D, Pistor T V and Stolz C J 2009 *Proc. SPIE* **7504** 75040M

[13] Qiu S R, Wolfe J E, Monterrosa A M, Feit M D, Pistor T V and Stolz C J 2011 *Appl. Opt.* **50** C373

[14] Salleo A 2001 *High-Power Laser Damage in Fused Silica* (PhD Dissertation) (Berkeley: University of California, Berkeley)

[15] Li J, Yang F Q, Wang Z and Dong J F 2011 *Acta Phys. Sin.* **60** 114104 (in Chinese)

[16] Li X L, Zhang L S, Sun J and Feng X M 2012 *Acta Phys. Sin.* **61** 044202 (in Chinese)